

BRANCHING PHOTOCYCLE OF SENSORY RHODOPSIN IN *HALOBACTERIUM HALOBIUM*

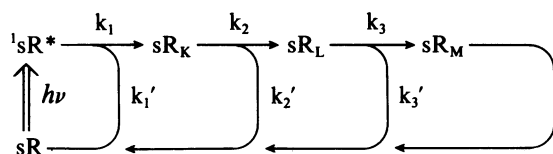
HIROYUKI OHTANI,* TAKAYOSHI KOBAYASHI,* AND MOTOYUKI TSUDA†

*Department of Physics, Faculty of Science, University of Tokyo, Hongo, Bunkyo-ku, Tokyo 113, Japan; and †Department of Physics, Sapporo Medical College, Chuo-ku, Sapporo 060, Japan

ABSTRACT Temperature effect of the photocycle of sensory rhodopsin (sR) was studied by nanosecond spectroscopy. Though the formation yield of sR_M (sR₃₇₀) was sharply decreased with temperature, those of sR_K (sR₆₈₀) and sR_L were insensitive to temperature changes. These results show the existence of the branching process back to sR from sR_L. The absorption maxima for sR_K and sR_L were 595 ± 5 and 555 ± 15 nm, respectively.

INTRODUCTION

Halobacterium halobium is attracted to 565-nm light and repelled by 370-nm light (1). A sensory rhodopsin (sR), which was previously called third rhodopsin-like pigment or slow rhodopsin, was found in *H. halobium* (2, 3), and it was assigned to be a photoreceptor for the phototaxis of the bacteria (4, 5). The peak of the absorption spectrum of sR is ~590 nm (2, 3, 6). Three intermediates, sR_K (sR₆₈₀ [3]), sR_L (7), and sR_M (sR₃₇₀ [2, 3]) have been found in the photocycle of sR. sR_M is a photoreceptor for the repellent phototaxis of this bacteria and has own photocycle through sR₅₁₀ (8, 9). It was shown that the chromophores of sR and sR_M are solely all *trans* and 13 *cis* retinals, respectively (8). Thus attractant and repellent phototaxis are triggered by the photoisomerizations of all *trans* and 13 *cis* retinals, respectively. As shown in the previous papers, the formation yield of sR_M decreases with temperature (10), though the formation yield of sR_K at 3.8°C is almost equal to that at 19.5°C (7). These results suggest that there are the following branchings in this photocycle, which recovers to the original pigments before sR_M.



Present study of the temperature effect on the formation yields of sR_K and sR_L strongly suggests that the branching process takes place between sR_L and sR_M, which might be analogous to the branching ($L \rightarrow M$ and $L \rightarrow bR_{570}$

processes) in the light-adapted bacteriorhodopsin (11, 12).

MATERIALS AND METHODS

Preparation of Sensory Rhodopsin

The calotenoid-free strain of *H. halobium* which is a mutant of F1x3 (bR⁻, hR⁻, sR⁺) was grown and harvested by standard methods (5, 13). After being washed three times with 4 M NaCl in 5 mM morpholino propane sulfonic acid (MOPS) (pH 7.2), envelope vesicles were obtained by sonication. The vesicles were suspended with 2 % (wt/vol) Tween-20 and incubated for 1 h at 4°C to remove the membranes solubilized by Tween-20. The suspension was centrifuged at 600,000 g for 1 h and washed twice with 4 M NaCl in 5 mM MOPS (pH 7.2). Then it was sonicated and centrifuged at 20,000 g for 10 min to reduce turbidity.

Nanosecond Time-resolved Spectroscopy

An excitation light source was the second harmonic (532 nm, 5-ns fwhm) of a Q-switched Nd:YAG laser (model DCR-1A, Quanta-Ray/Spectra Physics International, Mountain View, CA) or a dye laser (630 nm, 15-ns full width at half maximum, model TDL-III, Quantel International Inc., Santa Clara, CA) pumped by the second harmonic of a Q-switched Nd:YAG laser (model YG472, Quantel International Inc.). A xenon lamp (300 W, model VIX300F, Varian Associates, Palo Alto, CA, or 150 W, model L2274, Hamamatsu Photonics K. K., Hamamatsu, Japan) and a tungsten lamp (100 W, model Sylvania, Kondo, Tokyo, Japan) were used for the monitoring light sources for the measurement of the 10 ns–180 μs and 2 μs–45 ms time regions, respectively. The output signal of a photomultiplier (model R666S, Hamamatsu Photonics K. K.) was digitized by transient recorders (10–200 ns/point, nine bits, model DM901, Iwatsu K. K., Tokyo, Japan, or 1–50 μs/point, 12 bits, model HR1200, Kawasaki Electric Co., Tokyo, Japan) connected to an analysis system with a microcomputer (14, 15). Sample temperature was kept constant ($< \pm 0.5^\circ\text{C}$) with a water bath.

RESULTS AND DISCUSSION

Formations and Decays of Intermediates sR_K and sR_L

Fig. 1 shows the time-resolved difference spectrum of membrane suspension 2 μs after 532-nm excitation at

Dr. Ohtani's present address is Hamamatsu Photonics K. K. Tsukuba Research Laboratory, Tokodai, Tsukuba-shi, Ibaraki 300-26, Japan.

Correspondence should be addressed to Dr. Kobayashi.

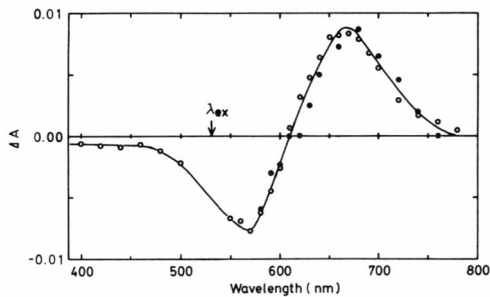


FIGURE 1 Time-resolved difference absorption spectrum of sR membrane suspension 2 μ s after the 532-nm excitation of 22.5°C (open circles) and at 3.5°C (solid circles). Signals obtained by 32 laser shots were averaged for each wavelength.

22.5°C (open circles) and at 3.5°C (solid circles). The peaks of negative and positive absorbance changes around 570 and 670 nm, respectively, are due to the bleaching of sR and the formation of a red-shifted intermediate sR_K, respectively. sR_K is formed within the resolution time (10 ns) of the apparatus at all temperatures between 3.5 and 33.0°C. The spectrum measured at 22.5°C (open circles) are nearly identical with that at 3.5°C (solid circles) and with that previously reported (7).

Open circles in Fig. 2 show the temperature dependence of the normalized formation yield of sR_K (η_K) determined from the absorbance change at 680 nm immediately after 532-nm excitation of membrane suspension. The yield is less sensitive to temperature change in the 3.5–33.0°C temperature region. We found that sR_K is converted to the next intermediate sR_L in the previous paper (7). The increase in absorbance due to the formation of sR_L was observed in the 500–540 nm region. The buildup time of the absorption in the wavelength region could not be determined because of the weak signal with smaller absorbance change than 7.5×10^{-4} .

The rate constant for the sR_K \rightarrow sR_L process was measured by monitoring the absorbance change at 680 nm and shown by solid circles in Fig. 3. The Arrhenius plot is composed of the two lines with different slopes above and below a transition temperature ($T = 23.5^\circ\text{C}$). Activation energies were 18 ± 4 kJ/mol and 114 ± 3 kJ/mol for

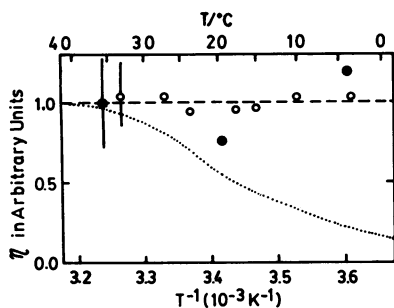


FIGURE 2 Temperature dependence of the normalized formation yields (η) for sR_K (open circles), sR_L (solid circles), and sR_M (dotted line, taken from reference 10).

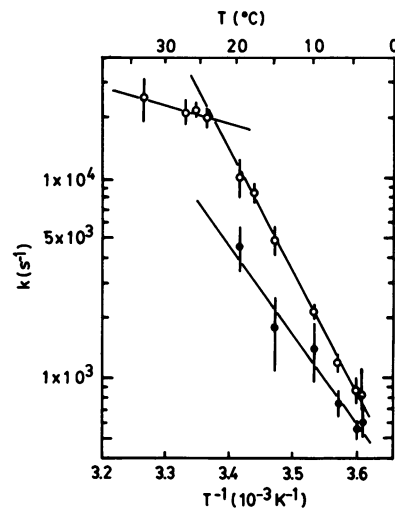


FIGURE 3 Rate constants for the decay of sR_K monitored at 680 nm ($k = k_2 + k'_2$, open circles) and the formation of sR_M monitored at 385 nm ($k = k_3 + k'_3$, solid circles).

temperature regions above and below T , respectively. Such discontinuity in the Arrhenius plots has been found in the kinetics of sR_M ($T = 15^\circ\text{C}$ [10]) and photointermediates of bacteriorhodopsin ($T = 25\text{--}32^\circ\text{C}$ [16]) and halorhodopsin ($T = 5^\circ\text{C}$ [10]). The transition temperature, 23.5°C , is not attributed to that for the intrinsic phase transition of the lipid layer. Tsuda et al. (17) reported that the transition temperature for native purple membrane is $\sim 42^\circ\text{C}$. A conformational change in sR may induce the lipid phase transition in the restricted small area in which lipid molecules interact with apoprotein.

sR_L is converted to sR_M (7). Closed circles in Fig. 3 show the temperature dependence of the formation rate of sR_M measured at 385 nm between 3.8 and 19.5°C. Here, the rate constant was obtained by the method described in Appendix A. The rate constant for the process as well as the sR_K \rightarrow sR_L process depends strongly on temperature. The activation energy was 75 ± 13 kJ/mol in the temperature region 3.5–19.5°C.

Recovery of sR from Intermediates

The formation yield of sR_M (η_M) decreases with temperature (10) (Fig. 2, dotted curve). There may be a recovery pathway to sR from sR_K and/or sR_L without forming sR_M as an intermediate between the two (7). The temperature dependence of the relative formation yield of sR_L [$\eta_L = \eta_K k_2 / (k_2 + k'_2)$] was estimated as follows. Details of the determination are described in Appendix B.

$$\eta_L(36.5^\circ\text{C}) : \eta_L(19.5^\circ\text{C}) : \eta_L(3.75^\circ\text{C}) \\ = (1.00 \pm 0.14) : (0.76 \pm 0.19) : (1.20 \pm 0.31)$$

Closed circles in Fig. 2 show that the formation yield η_L seems to be less sensitive to temperature change than η_M . Therefore, the decrease in the conversion efficiency from sR_L to sR_M [$\phi_3 = k_3 / (k_3 + k'_3)$] with temperature mainly

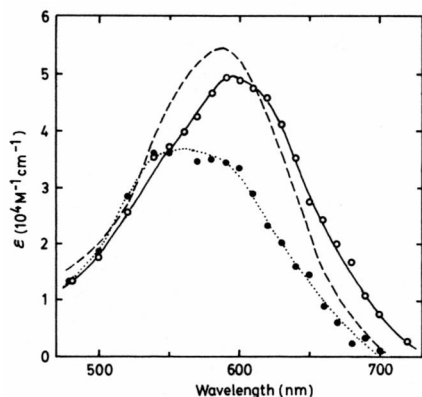


FIGURE 4 Absorption spectra of sR (dashed curve, taken from reference 6), sR_K (open circles), and sR_L (solid circles).

contributes to the decrease in the quantum yield of sR_M ($\eta_M = \eta_L \phi_3 = \eta_K \phi_2 \phi_3$). There is a recovery process from sR_L to sR, which is similar to the recovery from L to bR₅₇₀ in the photocycle of the light-adapted bacteriorhodopsin (11, 12).

Absorption Spectra of sR_K and sR_L

Fig. 4 shows the absorption spectrum of sR (dashed line) previously reported (6) and those of sR_K (open circles) and sR_L (solid circles) obtained in the present study on the following assumptions. (a) The conversion efficiency from sR_K to sR_L is unity. (b) The efficiency of the sR_L → sR process decreases with temperature. (c) The conversion efficiency from sR_K to sR_M is unity at 40°C. Details are described in Appendix C. The absorption maximum (λ_{max}) of sR_K (595 ± 5 nm) is slightly shifted from that of sR (587 nm [6]), and is similar to that of KL (596 nm [18]). The molar extinction coefficient at λ_{max} (ϵ_{max}) is smaller than that of sR. In the case of bacteriorhodopsin, it has been reported that ϵ_{max} of K (or KL) is larger than that of bR₅₇₀ (11, 18). Polland et al. (19) recently obtained the absorption spectrum of K. Their results show that ϵ_{max} of K is smaller than that of bR₅₇₀. The absorption spectrum of sR_L has a maximum in the 540–570 nm region, and it is similar to that of L (11, 18).

Conclusion

Photocycles of sR and bR₅₇₀ have the following common characters. (a) A photocycle is initiated by the rapid photoisomerization of retinal. (b) An intermediate (sR_K, K) with an absorption spectrum more red-shifted than that of the original pigment is formed in the early stage of the photocycle. (c) The red-shifted intermediate is converted to a slightly blue-shifted intermediate (sR_L, L). (d) A part of the secondary species directly forms the original pigment followed by a thermal isomerization of retinal (13 *cis* → all *trans*). (e) The other part of the species forms a metastable intermediate with a blue-shifted spectrum (sR_M, M). (f) The branching ratio between the two processes depends on temperature. At physiological tem-

perature sR_L and L are efficiently converted to sR_M and M, respectively. The sR_L → sR_M conversion may follow a deprotonation of retinal Schiff base which occurs in the L → M process.

APPENDIX A

The formation rate $\lambda_3 (= k_3 + k'_3)$ of sR_M was determined by the least-square fitting of the following equation to the observed absorbance change at 385 nm (ΔA_{385}).

$$\Delta A_{385}(t) = C_1 + C_2 \exp(-\lambda_2 t) + C_3 \exp(-\lambda_3 t) \quad (A1)$$

The value $\lambda_2 (= k_2 + k'_2)$ has been determined from the absorbance change at 680 nm.

APPENDIX B

The temperature dependent efficiency for the sR_K → sR_L conversion $\phi_2 [= k_2/(k_2 + k'_2)]$ was estimated from the following equation.

$$\phi_2 = [\Delta A(t) - \Delta A(0) \exp(-\lambda_2 t)] / (\epsilon^L - \epsilon^S) \cdot [1 - \exp(-\lambda_2 t)] C_0 l \quad (B1)$$

Here, ϵ^K , ϵ^L , and ϵ^S are molar extinction coefficients of sR_K, sR_L, and sR, respectively, at 580 nm. The decay rate constant and the concentration of the initially formed sR_K are denoted by k_2 and C_0 , respectively. The delay time t was set at 37 μs, 100 μs, and 1.2 ms which are equal to the 1/e lifetimes of sR_K at 36.5, 19.5, and 3.75°C, respectively.

APPENDIX C

Molar extinction coefficients of sR_K and sR_L were determined from the following procedure. The observed absorbance change at delay time t , $\Delta A(t)$, is given by Eq. C1.

$$\Delta A(t) = (\epsilon^K [sR_K] + \epsilon^L [sR_L] + \epsilon^M [sR_M] + \epsilon^S [sR]) l - A(t < 0) \quad (C1)$$

Here, ϵ^K , ϵ^L , ϵ^M , and ϵ^S are molar extinction coefficients of sR_K, sR_L, sR_M, and sR, respectively. The absorbance of the sample (before excitation) is denoted by $A(t < 0)$. The concentrations of the four species at delay time t are given by the solutions of differential equations C2–C5.

$$d[sR_K]/dt = -\lambda_2 [sR_K] \quad (C2)$$

$$d[sR_L]/dt = \phi_2 \lambda_2 [sR_K] - \lambda_3 [sR_L] \quad (C3)$$

$$d[sR_M]/dt = \phi_3 \lambda_3 [sR_L] \quad (C4)$$

$$d[sR]/dt = (1 - \phi_2) \lambda_2 [sR_K] + (1 - \phi_3) \lambda_3 [sR_L] \quad (C5)$$

Here, the efficiencies for the sR_K → sR_L and sR_L → sR_M conversions are denoted by $\phi_2 (= k_2/[k_2 + k'_2])$ and $\phi_3 (= k_3/[k_3 + k'_3])$, respectively. The molar extinction coefficients of sR_K were determined with Eqs. C6 and C7.

$$\Delta A(0) = (\epsilon^K - \epsilon^S) C_0 l \quad (C6)$$

$$C_0 = \Delta A(\infty) / \phi_2 \phi_3 (\epsilon^M - \epsilon^S) l \quad (C7)$$

Here, the conversion efficiency from sR_K to sR_M ($\phi_2 \phi_3$) was obtained by using the relative efficiency (10) on the assumption that $\phi_2 \phi_3$ is unity at 40°C. The molar extinction coefficients of sR and sR_M are given in reference 6. The determined ϵ^K was used for the calculation of ϵ^L with Eqs. C2–C5 on the assumption that ϕ_2 is unity.

The authors thank Dr. Masayuki Yoshizawa and Dr. Hisao Uchiki for their assistance in the construction of the data analysis system.

This work was supported in part by a Grant-in-Aid for Special Distinguished Research (56222005) and Special Research Project (60115004) to T. Kobayashi and by a Grant-in-Aid (6058022) to M. Tsuda from the Ministry of Education, Science, and Culture.

Received for publication 28 October 1987.

REFERENCES

1. Hildebrand, E., and N. Dencher. 1975. Two photosystems controlling behavioural responses of *Halobacterium halobium*. *Nature (Lond.)* 257:46–48.
2. Tsuda, M., N. Hazemoto, M. Kondo, N. Kamo, Y. Kobatake, and Y. Terayama. 1982. Two photocycles in *Halobacterium halobium* that lacks bacteriorhodopsin. *Biochem. Biophys. Res. Commun.* 108:970–976.
3. Bogomolni, R. A., and J. L. Spudich. 1982. Identification of a third rhodopsin-like pigment in phototactic *Halobacterium halobium*. *Proc. Natl. Acad. Sci. USA* 79:6250–6254.
4. Spudich, J. L., and R. A. Bogomolni. 1984. Mechanism of colour discrimination by a bacterial sensory rhodopsin. *Nature (Lond.)* 312:509–513.
5. Takahashi, T., M. Watanabe, N. Kamo, and Y. Kobatake. 1985. Negative phototaxis from blue light and the role of third rhodopsinlike pigment in *Halobacterium halobium*. *Biophys. J.* 48:235–240.
6. Spudich, J. L., and R. A. Bogomolni. 1983. Spectroscopic discrimination of the three rhodopsinlike pigments in *Halobacterium halobium* membranes. *Biophys. J.* 43:243–246.
7. Ohtani, H., T. Kobayashi, and M. Tsuda. 1986. Photocycle of sensory rhodopsin: a new precursor of sR₃₇₀. *Photobiochem. Photobiophys.* 13:203–208.
8. Tsuda, M., B. Nelson, C.-H. Chang, R. Govindjee, and T. G. Ebrey. 1985. Characterization of the chromophore of the third rhodopsinlike pigment of *Halobacterium halobium* and its photoproduct. *Biophys. J.* 47:721–724.
9. Takahashi, T., Y. Mochizuki, N. Kamo, and Y. Kobatake. 1985. Evidence that the long-lifetime photointermediate of S-rhodopsin is a receptor for negative phototaxis in *Halobacterium halobium*. *Biochem. Biophys. Res. Commun.* 127:99–105.
10. Hazemoto, N., N. Kamo, Y. Terayama, Y. Kobatake, and M. Tsuda. 1983. Photochemistry of two rhodopsinlike pigments in bacteriorhodopsin-free mutant of *Halobacterium halobium*. *Biophys. J.* 44:59–64.
11. Iwasa, T., F. Tokunaga, and T. Yoshizawa. 1980. A new pathway in the photoreaction cycle of trans-bacteriorhodopsin and the absorption spectra of its intermediates. *Biophysics of Structure and Mechanism*. 6:253–270.
12. Kalisky, O., M. Ottolenghi, B. Honig, and R. Korenstein. 1981. Environmental effects on formation and photoreaction of the M₄₁₂ photoproduct of bacteriorhodopsin: implications for the mechanism of proton pumping. *Biophys. J.* 20:649–655.
13. Spudich, E. N., and J. L. Spudich. 1983. Control of transmembrane ion fluxes to select halorhodopsin-deficient and other energy-transduction mutants of *Halobacterium halobium*. *Proc. Natl. Acad. Sci. USA* 79:4308–4312.
14. Iwai, J., M. Ikeuchi, Y. Inoue, and T. Kobayashi. 1984. Early processes of protochlorophyllide photoreduction as measured by nanosecond and picosecond spectrophotometry. In *Protochlorophyllide Reduction and Greening*. C. Sironval and M. Brouers, editors. Martinus Nijhoff/Dr W. Junk Publishers, Hague. 99–112.
15. Ohtani, H., T. Kobayashi, T. Ohno, S. Kato, T. Tanno, and A. Yamada. 1984. Nanosecond spectroscopy on the mechanism of the reduction of methyl viologen sensitized by metallophthalocyanine. *J. Phys. Chem.* 88:4431–4435.
16. Korenstein, R., W. V. Sherman, and S. R. Caplan. 1976. Kinetic isotope effects in the photochemical cycle of bacteriorhodopsin. *Biophysics of Structure and Mechanism*. 2:267–276.
17. Tsuda, M., R. Govindjee, and T. G. Ebrey. 1983. Effects of pressure and temperature on the M412 intermediate of the bacteriorhodopsin photocycle. Implications for the phase transition of the purple membrane. *Biophys. J.* 44:249–254.
18. Shichida, Y., S. Matuoka, Y. Hidaka, and T. Yoshizawa. 1983. Absorption spectra of intermediates of bacteriorhodopsin measured by laser photolysis at room temperatures. *Biochim. Biophys. Acta* 723:240–246.
19. Polland, H.-J., M. A. Franz, W. Zinth, W. Kaiser, E. Kölling, and D. Oesterhelt. 1986. Early picosecond events in the photocycle of bacteriorhodopsin. *Biophys. J.* 49:651–662.